Environ. Sci. Technol. **2010,** *44,* 1683–1689

Estimation of In-Canopy Ammonia Sources and Sinks in a Fertilized *Zea mays* Field

JESSE O. BASH,*,† JOHN T. WALKER,‡ GABRIEL G. KATUL,§ MATTHEW R. JONES,‡ EIKO NEMITZ,|| AND WAYNE P. ROBARGE⊥

National Exposure Research Laboratory, U.S. Environmental Protection Agency, Research Triangle Park, North Carolina 27711, National Risk Management Research Laboratory, U.S. Environmental Protection Agency, Research Triangle Park, North Carolina 27711, Nicholas School of the Environment, Duke University, Durham, North Carolina 27708-0328, Centre for Ecology and Hydrology (CEH) Edinburgh, Bush Estate, Penicuik, EH26 0QB, United Kingdom, and Department of Soil Science, North Carolina State University, Raleigh, North Carolina 27695

Received December 9, 2009. Accepted January 8, 2010.

An analytical model was developed to describe in-canopy vertical distribution of ammonia (NH_3) sources and sinks and vertical fluxes in a fertilized agricultural setting using measured in-canopy mean NH_3 concentration and wind speed profiles. This model was applied to quantify in-canopy air−surface exchange rates and above-canopy NH_3 fluxes in a fertilized corn (*Zea mays*) field. Modeled air−canopy NH_3 fluxes agreed well with independent above-canopy flux estimates. Based on the model results, the urea fertilized soil surface was a consistent source of NH_3 one month following the fertilizer application, whereas the vegetation canopy was typically a net NH_3 sink with the lower portion of the canopy being a constant sink. The model results suggested that the canopy was a sink for some 70% of the estimated soil NH_3 emissions. A logical conclusion is that parametrization of within-canopy processes in air quality models are necessary to explore the impact of agricultural field level management practices on regional air quality. Moreover, there are agronomic and environmental benefits to timing liquid fertilizer applications as close to canopy closure as possible. Finally, given the large within-canopy mean NH_3 concentration gradients in such agricultural settings, a discussion about the suitability of the proposed model is also presented.

1. Introduction

Over the past three decades, interest in measuring and modeling bidirectional exchanges of NH_3 between the biosphere and the atmosphere has proliferated for a number of reasons. NH_3 plays a primary role in aerosol formation because it is an atmospheric acid-neutralizing agent. Atmospheric ammonium nitrate and ammonium sulfate aerosol adversely influences human health (*1*), decreases visibility, and affects atmospheric radiative forcing (*2*). NH_3 deposition also adversely affect ecosystems by contributing to soil acidification and habitat loss related to excess nutrient loading (*3*). Biological processes in soils enriched by reduced nitrogen (NH_x) deposition can lead to emissions of NH_3 and nitrous oxide, a greenhouse gas (*3*), and vegetation can act as a sink or source of atmospheric NH_3 (*4*). The use of NH_x as a fertilizer in agricultural processes has dramatically increased over the past century, and the trend is expected to continue with an increasing demand for biofuels and to simply meet the nutritional requirements of an increasing global population (*5*).

The impact of human activity on the nitrogen cycle has made the parametrization of NH_3 emissions and deposition in air quality models an active area of research for determining sound regulatory scenarios for human exposure to particulates, ecosystem nutrient loading, and climate change (*2*). The largest sources of atmospheric NH_3 are large-scale livestock operations and fertilized agricultural fields (*3*). Recent research has led to the development of mechanistic models to describe emissions from livestock operations (*6*) and air−vegetation NH_3 exchange (*7*). However, the role of vegetation in regulating NH_3 emissions from fertilized agricultural fields remains a subject of research (*8*) that lacks analytical tractability and a clear organizing framework for evaluating field measurements.

A process level understanding of biological, chemical, and mechanical processes influencing the soil−vegetation−atmosphere exchange of nitrogen over a variety of managed and natural ecosystems remains needed before the impact of field scale mitigation strategies on regional air quality can be realized (*9*). Progress has recently been made in elucidating the mechanisms driving NH_3 air−surface exchange. Bidirectional NH_3 exchange models that include stomatal compensation points, the equilibrium surface concentration when there is no net exchange, and parametrization of dynamic leaf surface chemistry models have been developed (*7, 10*−*12*) and adapted in a number of applications (*13*). Also, a process-based understanding of NH_3 exchange across atmospheric−stomatal cavity and atmospheric−vegetation surface interfaces has been proposed (*8*). Nevertheless, the effect of soil emission processes and alteration of in-canopy sources and sinks by enriched NH_3 concentration in these deeper layers of the canopy remain vexing research problems to be confronted (*2*).

Above-canopy NH_3 fluxes can be estimated using micrometeorological techniques, flux gradient approaches (*6, 14*), relaxed eddy accumulation (*15, 16*), or directly measured via eddy covariance methods (*17*). Such measurements are a net soil−canopy−atmosphere flux and do not distinguish between soil and vegetation contributions needed to advance model development (*2*). In-canopy sources and sinks of NH_3 enriched in a stable isotope of nitrogen have been made by using flux chambers (*12*), though the small scale of such measurements are "cursed" by large spatial variability.

Canopy-scale sources, sinks, and fluxes may be inferred based on an "inversion" using in-canopy mean scalar concentration profile measurements (*18*−*21*). Two broad "inversion" approaches exist; Eulerian-based closure schemes that vary in complexity (e.g., refs *22*−*28*) and Lagrangian near field (LNF) dispersion models (*23, 29, 30*). Higher order Eulerian methods generally require measurements or modeling of the in-canopy flow field, but more important, they require the turbulent kinetic energy dissipation rate or the relaxation time scale profiles. These quantities are notoriously

* Corresponding author.
† National Exposure Research Laboratory.
‡ National Risk Management Research Laboratory.
§ Duke University.
|| Centre for Ecology and Hydrology (CEH) Edinburgh.
⊥ North Carolina State University.

10.1021/es9037269 © 2010 American Chemical Society
Published on Web 01/27/2010

difficult to model or measure inside dense canopies. Likewise, LNF requires knowledge of vertical distributions of Lagrangian time scales and vertical velocity standard deviation. Uncertainties in these parameters can lead to unrealistic integrated flux profiles (*19, 31*). To date, a simplified analytical method that can explicitly predict canopy sources and fluxes of NH_3 from mean concentration profiles is desirable but lacking, though interest in this topic is gaining popularity in canopy turbulence research (*32*).

Here, we propose a simplified analytical model that describes the in-canopy vertical distribution of NH_3 sources and sinks and vertical fluxes in a fertilized agricultural setting aimed at quantifying in-canopy air−surface exchange and above-canopy NH_3 flux. While simplified analytical models can be criticized "ad-infinitum", especially when they are theoretically anchored to first-order closure principles, the technique proposed here provides constraints that allow above-canopy fluxes, soil and leaf chemistry measurements, and measurements of environmental variables to be interpreted. The fact that this approach is applied to a fertilized agricultural setting often characterized by large mean vertical gradients in NH_3 concentrations permits some theoretical justification for the usage of first-order closure principles. Performance of the model was also evaluated against direct eddy covariance measurements of sensible heat fluxes and modified Bowen ratio (MBR) fluxes of above canopy NH_3 fluxes collected at the field site.

2. Experimental Section

2.1. Site Description. The site was a 200 ha agricultural field near Lillington, North Carolina (35° 22′ 35.7" latitude 78° 46′ 45.1" longitude 45 m elevation). Soils were primarily fine sandy loam (Exum series) with a texture of 21, 68, and 11% sand, silt, and clay, respectively. Beneath the canopy, the ground surface was primarily exposed soil with little leaf litter. The field was planted in corn (*Zea mays*, Pioneer varieties 31G66 and 31P41, density of ≈70 000 plants ha^{-1}) and fertilized with 50 kg N ha^{-1} ammonium polyphosphate (injected) between 4/18/07 and 4/23/07. The field was fertilized again between 5/25/07 and 5/29/07 with 135 kg N ha^{-1} urea ammonium nitrate solution (surface applied) containing Agrotain nitrogen stabilizer. The canopy reached a peak leaf area index (single-sided) of 2.9 ± 0.6 m^2 m^{-2} and a maximum canopy height (h_c) of 2.2 m near 7/15/07 and had fully senesced by 8/21/07.

2.2. In-Canopy Measurements. In-canopy mean velocity, air temperature and NH_3 concentration profiles were measured from July 6 through August 1, 2007. An ATI 3D sonic anemometer (Applied Technologies, Inc., Longmont, CO) was mounted on an adjustable bracket to measure sensible heat and momentum fluxes within the canopy. The sonic anemometer was sampled at 10 Hz and mounted from 0.5 to 1.5 m above the soil surface. In-canopy NH_3 concentrations were measured using duplicate phosphorous acid coated annular denuders (URG, Chapel Hill, NC) mounted at 0.1, 0.3, 0.95, 1.5, and 2.25 m above ground level. Denuders were sampled for approximately two hours each at an air flow rate of 20 L min^{-1}. After sampling, denuders were extracted with 2.5 mL deionized water and analyzed for NH_4^+ by ion chromatography (model DX120, Dionex Corporation, Sunnyvale, CA). Air concentrations (μg NH_3 m^{-3}) were calculated by dividing the mass of NH_3 collected by the total volume of air sampled. Excellent precision was achieved between paired in-canopy denuder replicates; the median relative difference was 4.6% ($N = 45$). Each denuder set was collocated with a copper-constantan thermocouple sampled at a frequency of 1 Hz. Leaf temperatures were sampled at 1 Hz using copper-constantan thermocouples affixed to the leaf surfaces at 0.65, 0.85, 1.4, 1.8, and 1.8 m above the ground. Apoplastic [NH_4^+] and pH were measured from extracted leaf apoplastic solution by using the vacuum infiltration technique (*33*) to directly measure the canopy's emission potential.

2.3. Above-Canopy Measurements. R.M. Young model 81000 sonic anemometers (R.M Young Company, Traverse City, MI) were mounted at 2.5, 3.5, and 10 m above the ground level and a leaf wetness sensor was mounted at the canopy height (Campbell Scientific, model 237, Logan, UT). Four collocated phosphorous acid coated denuders (URG, Chapel Hill, NC) mounted at 4.92 m above the soil surface were sampled for twelve hours each at an air flow rate of 10 L min^{-1}. Vertical NH_3 concentration gradients above the canopy were measured at 0.3 and 2.4 m above the canopy with a continuous flow wet denuder system "AMANDA" (ammonia measurement by annular denuder sampling with online analysis; ref *14*). Gaseous NH_3 was collected from the sample airstream (30 L min^{-1}) in a wetted continuous-flow annular denuder using a stripping solution of 3.6 mM $NaHSO_4$. The aqueous NH_3 concentration was determined by a detector based on a selective ion membrane and online conductivity analysis (detection limit ≈ 0.02 μg NH_3 m^{-3}) by sequentially sampling each denuder such that a vertical profile was determined every 15 min for 30 min flux calculations. Copper-constantan thermocouples were collocated with annular denuders to measure ambient mean air temperature profiles.

2.4. Modified Bowen Ratio for Above-Canopy Fluxes. Above-canopy NH_3 fluxes were estimated using the modified Bowen ratio (MBR) method. The MBR method assumes the turbulent diffusivity of NH_3 is similar to the turbulent diffusivity of heat such that

$$F_{NH_3} = \overline{w'T'}\frac{\Delta\bar{C}}{\Delta\bar{T}} = \overline{w'T'}\frac{\bar{C}(z_1) - \bar{C}(z_2)}{\bar{T}(z_1) - \bar{T}(z_2)} \quad (1)$$

where F_{NH_3} is the air−canopy flux of NH_3, $\overline{w'T''}$ the eddy-covariance measured sensible heat flux and, $\Delta\bar{C}$ and $\Delta\bar{T}$ are colocated mean NH_3 concentration and air temperature measured differences at heights z_1 and z_2.

2.5. Analytical First-Order Closure Model for In-Canopy Fluxes. The mean in-canopy continuity equation for a stationary and planar-homogeneous high Reynolds number flow in the absence of subsidence can be expressed as

$$\frac{\partial\bar{C}}{\partial t} = -\frac{\partial\overline{w'C'}}{\partial z} + S(z) = 0 \quad (2)$$

where C is a scalar concentration (e.g., NH_3), $\overline{w'C'}$ is the scalar flux and $S(z)$ is the source/sink rate of C. The scalar flux can be estimated using gradient-diffusion (K) theory;

$$\overline{w'C'} = -K_e\frac{\partial\bar{C}}{\partial z} \quad (3)$$

where K_e is the eddy diffusivity for NH_3. While first order closure models are often questionable inside canopies (*29*), this approximation may be valid for NH_3 under conditions associated with fertilized cropping systems where NH_3 concentration profiles would be expected to decrease monotonically with height (Supporting Information (SI) Text S1). In-canopy eddy diffusivity can be characterized from the mean wind speed profile and the mixing length hypothesis via

$$K_e = \frac{1}{Pr}L_m^2\left|\frac{\partial\bar{U}}{\partial z}\right| \quad (4)$$

where L_m is the mixing length, and Pr is the turbulent Prandtl number (*34*). Pr is near unity for near-neutral flows in the atmospheric surface layer (ASL); however, values as low as 0.5 have been reported near the canopy top (*35*).

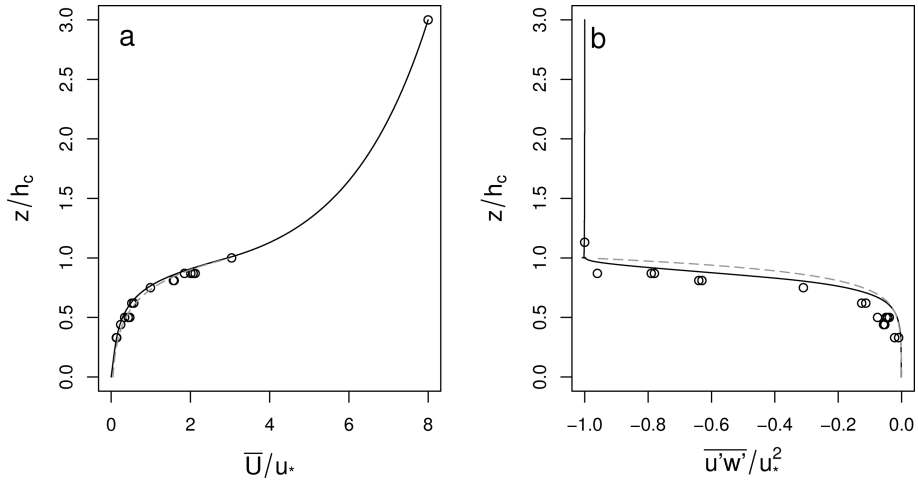

FIGURE 1. Comparison between measured and modeled normalized mean wind speed and momentum flux profiles. The data are from Wilson (*47*) (circles) and K-ε model (black line) and the analytical model (dashed gray line) estimates of the mean wind speed normalized by u_*(a) and the Reynolds' stress normalized by $u_*^2$are plotted as a function of height normalized by canopy height (b).

The mixing length is parametrized following Harman and Finnigan (*34*):

$$L_m = \frac{2\beta^3}{C_d a(z)\varphi_m\left(\frac{h_c - d}{L}\right)} \tag{5}$$

where β is the dimensionless momentum flux ($u_*/\bar{U}|_{z=h_c}$), C_d is the product of the in-canopy drag coefficient and the sheltering factor (typically between 0.1 and 0.3 (*36*)), a is the mean leaf area density, the ratio of the plant area index to the canopy height (h_c), d is the zero plane displacement, L is the Obukhov length, and φ_m is the dimensionless correction factor for atmospheric stability.

The in-canopy mean wind speed profile, turbulent diffusivity for momentum ($K_t = K_e$Pr), and momentum flux ($\overline{u'w'}$)are based on the analytical solution of Inoue (*37*) following the parametrization of Harman and Finnigan (*34*):

$$\begin{aligned} \bar{U}(z) &= \bar{U}(h_c)\exp\left[\frac{\beta(z - h_c)}{L_m}\right]_{z<h_c} \\ K_t &= \beta L_m \bar{U}(z) \\ \overline{u'w'} &= -(\beta \bar{U}(z))^2 \end{aligned} \tag{6}$$

The above-canopy stability corrected log−linear mean wind speed profile was used to scale the wind speed measured at 2.5 and 3.5 m to the canopy height ($z = h_c$) following Byun (*38*)

$$\bar{U}(z) = \frac{u_*}{k}\left(\ln\left[\frac{z - d}{z_o}\right] + \psi\left(\frac{z - d}{L}\right) - \psi\left(\frac{z_0}{L}\right)\right)_{z/h_c>1} \tag{7}$$

where z_o is the momentum roughness length, d is the zero plane displacement (0.1 h_c and $^2/_3$ h_c respectively), $k = 0.4$ is von Karman's constant, and ψ is the integrated diabatic stability correction.

Upon substituting these approximations into eq 2, the NH_3 sources and sinks are now analytically linked to the measured mean concentration profile, momentum absorption by the canopy drag elements, mixing length, and the friction velocity at the canopy top via

$$S(z) = \begin{cases} -\frac{u_*}{\mathrm{Pr}}\exp\left[\beta\left(\frac{z - h_c}{L}\right)\right]\left(L_m\frac{\partial^2\bar{C}}{\partial z^2} + \beta\frac{\partial\bar{C}}{\partial z}\right); z/h_c \le 1 \\ 0; z/h_c > 1 \end{cases} \tag{8}$$

The turbulent fluxes can be inferred by integrating eq 2 after solving eq 8 using measured mean concentration profiles.

Results and Discussion

3.1. Wind Profiles. Because the vertical variation of the momentum eddy diffusivity is central to the description of $S(z)$, the analytical model for mean velocity and turbulent stress was compared to the Wilson (*39*) data for a similarly structured corn canopy (LAI = 2.9, h_c = 2.21 m) (Figure 1). For reference, K-ε model results described in Katul et al. (*36*) are also shown in Figure 1. Both the analytical and K-ε models captured the variations well in wind speed profiles measured by Wilson (*39*), with coefficient of determination (r^2) values of 0.987 and 0.989, respectively. When the analytical model was applied to field data, a clear underestimation in the measured in-canopy wind speed profiles under stable conditions emerged using the a priori specified drag coefficient (C_d = 0.3) of Wilson (*39*).

The best estimate of the wind profile over a variety of stability regimes was found when the in-canopy drag coefficient was solved from the parametrization of the in-canopy momentum flux, eqs 5 and 6, and measured momentum fluxes. The parametrization of a vertically invariant in-canopy drag coefficient is reasonable for a corn canopy, known to have a relatively uniform vertical distribution of leaf area densities and closed understory. However if this formulation is to be applied for a canopy with an open understory and more variable leaf area density, the drag coefficient should be parametrized as a function of height (*40*, *41*).

3.2. Turbulent Sensible Heat Flux Estimation. Sensible heat fluxes estimated by integrating the source−sink profile of the analytical closure model from the soil surface ($z = 0$) up to the canopy height ($z = h_c$) correlate well with measured sensible heat fluxes. Comparison of above-canopy fluxes by regression analysis indicates a linear relationship with a slope of 1.05 and intercept of -8.30×10^{-3} °C m s^{-1} (r^2 = 0.854, $p < 0.001$, N = 341); mean normalized bias and error are −21 and 50%, respectively. Comparison of in-canopy measured and modeled fluxes yields a slope of 0.646 and intercept of -1.72×10^{-3} °C m s^{-1} ($r^2 = 0.632$, $p < 0.001$, N = 341) with mean normalized bias and error of −49 and 59%, respectively (Figure 2). Above-canopy sensible heat fluxes were underestimated during the morning transition when the upper canopy was being heated and overestimated during the evening transition when the upper canopy was cooling (when stationarity assumptions are questionable). In-canopy sensible heat fluxes were underestimated during the midday

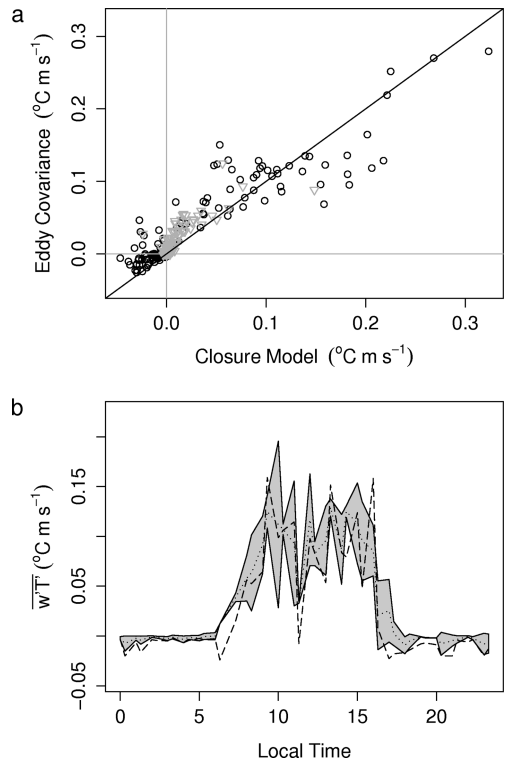

FIGURE 2. Scatter plot of measured and integrated modeled kinematic sensible heat fluxes, $\overline{w'T'}$ at the canopy top (black circles) and in the canopy (gray triangles, $z/h_c = 0.23-0.68$) (a). Hourly averages of eddy covariance (dotted line) and closure model (dashed lines) sensible heat fluxes are shown. The shaded area represents ±1 standard deviation bounds from the eddy covariance flux measurements (b).

peak, possibly because the model does not consider soil heat storage (see SI Text S1).

It is important to note that, while the sensible heat flux is commonly used to evaluate in-canopy source/sink models, in this case such a comparison may represent a worst case test of the model. The first-order approach presented here should perform best when a large monotonic gradient is present. As described in SI sections S1 and S2, the measured NH_3 concentration gradients are always much larger than the corresponding temperature gradients. While the agreement between measured and modeled heat fluxes presented here is comparable to and in some cases exceeds the performance of other Eulerian and LNF techniques (*22*−*30*) in different canopies, it may not be truly indicative of the skill of the proposed method. Comparison to the flux of a nonreactive compound such as N_2O, which is emitted only from the soil and at similar rates to NH_3, would be more appropriate.

3.3. Air−Canopy Ammonia Flux Estimates. Measured in-canopy NH_3 concentration profiles were consistently near monotonic during all in-canopy sampling periods with the magnitude of the concentration decreasing with height from the soil surface to the top of the canopy suggesting that first-order closure principles may be applicable (SI Text S1, Figure 3). In-canopy concentration profiles where separated into three categories; (1) included samples that were taken before sunrise when the atmosphere was typically stable (Figure 3a), (2) included samples that were taken in mid to late morning during the canopy drying period (Figure 3b), and (3) included samples that were taken from late morning into the afternoon when the canopy was typically dry and conditions were unstable (Figure 3c). Above canopy NH_3 fluxes estimated by integrating modeled in-canopy source sink profiles from the soil surface to the canopy height compared well (regression slope = 0.882, significant at $p < 0.001$ and the intercept was not statistically different from 0) with above canopy MBR flux measurements (Figure 4). When the largest evasive flux measured on July sixth was removed from the analysis the slope dropped to 0.386 but the correlation was still significant at $p < 0.05$ and the least-squares regression line falls within the 95% confidence interval, based on the variability of the flux in each sampling period, of six of the remaining eight sets of MBR flux measurements.

3.4. In-Canopy NH_3 Sources and Sinks. In-canopy source/sink and concentration profiles indicate that, approximately one month following fertilizer application, the canopy recaptures the majority NH_3 emitted from the soil surface. On average, 73% of soil NH_3 emissions were taken up by the canopy at a mean rate of 118 ng m^{-2} s^{-1}. Canopy uptake was similar in magnitude to the sugar cane crop studied by Denmead et al. (*18*); however, the fractional uptake of estimated soil emissions was much greater for this site. Soil emissions estimates and mean concentration measurements of Denmead et al. (*18*) were 1−2 orders of magnitude higher than presented here. The difference in the uptake of soil emissions may be influenced by differences in the in-canopy ambient NH_3 concentrations and fertilization rates, which drive the stomatal component of the foliage exchange through the regulation of apoplast chemistry and, subsequently, the stomatal compensation point.

Net canopy compensation points, which represent the combined effects of cuticular and stomatal exchange, were approximated by inverting the modeled source sink profiles. This inversion is analogous to the technique applied to the LNF modeled sources and sinks of Harper et al. (*42*). Upper canopy (i.e., $0.5 < z/h_c \leq 1$) modeled compensation point compared well with experimentally derived stomatal compensation points estimated from measured leaf temperature and apoplast NH_4^+ and H^+ concentrations (mean of 2.31 μg m^{-3} and 2.13 μg m^{-3} respectively). Exchange in the upper canopy was also bidirectional depending on the strength of the soil emissions, above canopy concentrations, and environmental parameters (e.g., leaf wetness, leaf temperature, relative humidity, etc.). This result is in good agreement with above canopy MBR measurements of Nemitz et al. (*15*) despite differences in the ground surface emissions sources (Table 1). Ground surface emissions were from fertilizer application here and from senescent leaves in Nemitz et al. (*15*). Deeper in the canopy ($0 < z/h_c < 0.5$), the sinks remain persistent through daytime and early morning hours when stomatal exchange is expected to be small suggesting that cuticular processes dominate uptake in these lower canopy layers, while the stomatal component of the net air−surface exchange is relatively more important in the upper canopy layers. Modeled canopy compensation points were approximately half of the values for *Z. mays* reported by Harper and Sharpe (*21*) and at least an order of magnitude lower than those estimated by Harper et al. (*42*) using the LNF dispersion technique, although these studies also reported ambient concentrations at least an order of magnitude larger than those measured here.

In-canopy source/sink estimates for stable nighttime conditions indicate a net NH_3 deposition to the canopy, in agreement with above-canopy MBR fluxes. In-canopy concentrations increased through early morning sampling, during stable periods, peaking at approximately 9:30 a.m. and then decreasing during late morning and afternoon hours presumably through venting of the canopy (Figure 3; SI Text S2). This observation is consistent with the observations of Nemitz et al. (*19*) in an oilseed rape (*Brassica napus*) canopy, where ground surface emissions from decomposing senesced leaves escaped the canopy only during windy nighttime conditions.

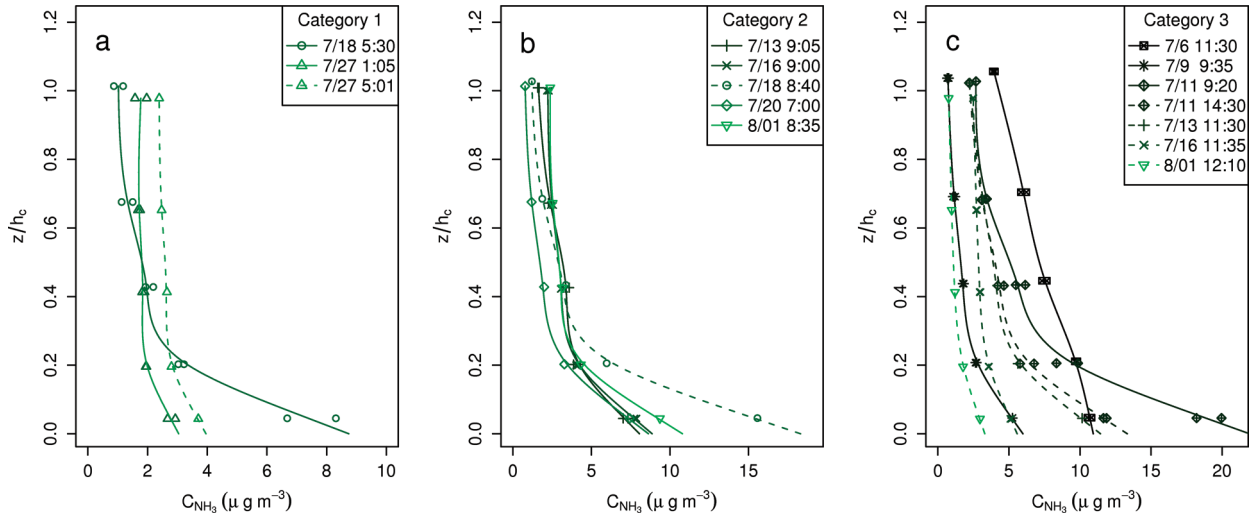

FIGURE 3. Measured NH_3 concentration profiles (C_{NH_3}) from July 6 to August 1 for in-canopy sampling periods before (a), during (b), after (c) the time frame of the average morning concentration peak. The lines indicate smoothed concentration profiles needed in first and second derivative estimations when determining the source/sink profile (*S*).

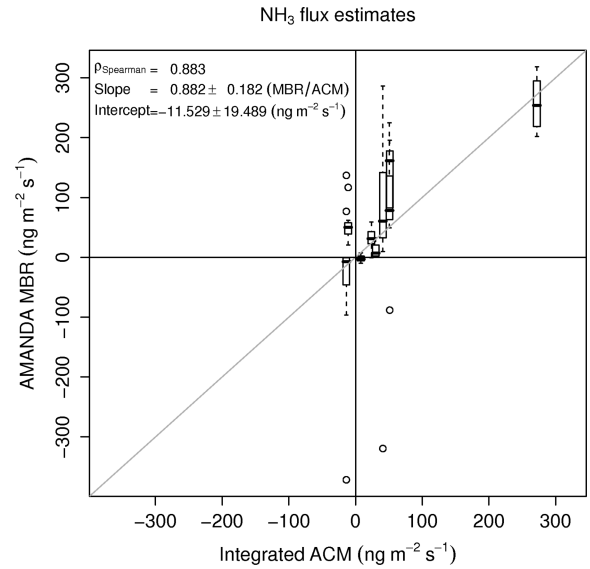

FIGURE 4. Above canopy modified Bowen ratio NH_3 (AMANDA MBR) flux vs the NH_3 flux derived from integrating the analytical closure model (ACM) *S* to the canopy top (Integrated in-canopy).

A diel morning peak in above canopy ambient NH_3 concentrations and evasive MBR flux measurements, beginning at approximately 7:00 a.m. EST to a mean daily maximum at approximately 8:00 a.m. EST, was persistent during the month of in-canopy sampling (Figure 5). Leaf drying experiments were conducted to investigate if the morning "spike" in mean NH_3 concentrations was, in part, due to the evasion of ammonium contained in dew droplets as the canopy dried. The average concentration of NH_4^+ in the leaf surface droplets was 689 μg L^{-1} (and ranged from 11 to 2989 μg L^{-1}). During the leaf drying experiments, we measured 25−35 g H_2O m^{-2} leaf area in the upper and middle canopy (with widely varying but smaller amounts in the lower canopy). Assuming a leaf area of 3.0 m^2 m^{-2} and further assuming that the canopy dries completely between sunrise and 9:30 a.m. (based on our measurements), an average emission flux 4.0 ng NH_3 m^2 s^{-1} was calculated for the drying period. Using the maximum observed NH_4^+ concentration in dew water yields an estimated maximum emission during the drying of the canopy of 17.6 ng NH_3 m^2 s^{-1}, 5−21% of the median MBR flux of 84.7 ng NH_3 m^2 s^{-1} measured between 7 a.m. and 10 a.m. EST from July 6th through August 1st. The direction of the NH_3 flux estimation and concentration of NH_4^+ in the dew indicate that the peak in the morning NH_3 concentrations originated primarily from canopy and soil sources rather than dew as observed by Sutton et al. (*10*).

Closure model estimates of the evasion of NH_3 from the soil surface were assumed to be equal to the source/sink estimate at $z = 0$. This estimate is independent of soil physical and chemical processes and is based on the near soil surface concentration profile and model estimated eddy diffusivity constrained by the in-canopy measurements extrapolated to the soil surface using the first order closure model. Results indicate that the large in-canopy concentration gradient was driven by persistent emissions from the urea fertilized soil surface throughout the measurement period (Table 1, SI Figure S3). Soil surface emission and canopy uptake estimates were enhanced by rainfall (*43*) in agreement with Roelle and Aneja (*44*). Accumulation of NH_3 on vegetative surfaces has been shown to reduce canopy uptake (*17, 45*) and enhanced uptake of NH_3 following precipitation may be due to wash-off. However, air motion and transport processes remain uncertain near the soil surface because, as in other in-canopy studies, measurements were not made near the soil surface ($z < 0.5$ m) due to the 0.1 m path length and sampling frequency of the sonic anemometer (*19*). The structure of the boundary layer near the soil surface is unresolved and typically ignored due to difficulties in measuring wind and scalar variables (*46*) at appropriate spatial and temporal scales. Estimates of the in canopy air−soil flux from the closure model include uncertainty in the extrapolation of the in-canopy exchange parametrizations to the soil surface. However, these uncertainties are also present for LNF and more complex Eulerian closure models and the presence of a strong near-monotonic measured concentration profile indicate that the soil was a local source of NH_3 emissions.

3.5. Field and Regional Scale Applications. On average, 26.8% of the emissions from the ground level were estimated to be released to the atmosphere. Thus, there are agronomic and environmental benefits to timing fertilizer applications as close to canopy closure as possible while considering the physiological nitrogen requirements of the crop (*47, 48*).

The use of an analytical in-canopy source/sink model is useful in applying constraints to the relative contributions of vegetation and soil to net canopy-scale fluxes of NH_3. This closure technique is more constrained by measurements than a priori specified empirical resistances to partition above canopy fluxes into contributions from canopy and soil

TABLE 1. Canopy flux, Uptake and Compensation Point Estimates and Meteorological Conditions, Where T_a is the Mean Ambient Temperature at the Canopy Top, T_L is the Mean Leaf Temperature, T_s is the Mean Soil Temperature at $z = -5$ cm, RH is the Relative Humidity, and Γ Is the Leaf Emission Potential at the Canopy Height Assuming the Flux Is Stomatally Controlled

date	time	soil flux[a] ng m^{-2} s^{-1}	net flux[a] ng m^{-2} s^{-1}	canopyflux[a] ng m^{-2} s^{-1}	$U(h_c)$ m/s	$u^a(h_c)$ m/s	h_c/L m/m	canopy wetness % time	T_a °C	T_L °C	T_s °C	RH %	comp point μg m^3	$\Gamma[NH_4^+]/[H^+]$
6-July[3]	11:30−14:00	13.7	275	258	1.61	0.328	−0.255	0.0	31.68	34.76	29.46	48.35	7.43	370
9-July[3]	9:35−12:45	185	39.6	−146	1.316	0.262	−0.333	0.0	31.04	37.11	28.62	55.56	0.95	40
11-July[3]	9:20−14:15	308	−13.8	−322	2.764	0.54	−0.002	0.7	31.74	32.67	28.57	53.55	2.01	125
11-July[3]	14:30−17:40	281	41.0	−240	2.949	0.553	−0.003	3.6	30.05	29.84	29.57	61.41	1.48	125
13-July[2]	9:05−11:15	132	53.0	−81.1	1.214	0.251	0.125	32.6	26.69	26.46	25.97	51.09	2.87	354
13-July[3]	11:35−14:30	58.6	51.8	−7.3	1.031	0.206	−0.178	8.0	27.66	29.37	26.91	44.34	3.34	298
16-July[2]	9:00−11:15	189	7.97	−181	1.952	0.386	−0.064	0	28.43	30.67	26.35	64.79	1.04	81
16-July[3]	11:35−14:30	144	24.0	−120	1.741	0.347	−0.093	0	30.40	31.62	28.11	56.67	1.03	72
18-July[1]	5:30−8:20	53.4	29.7	−23.1	1.132	0.216	−0.047	100	21.15	22.37	24.94	93.05	2.18	429
18-July[3]	8:40−11:40	558	−11.0	−569	1.555	0.318	−0.231	NA	28.16	NA	27.07	71.25	2.24	229
20-July[2]	7:00−10:00	111	1.93	−109	1.556	0.274	−0.126	2	28.00	NA	25.95	64.03	2.26	235
27-July[1]	1:05−4:42	9.48	−4.18	−14.3	0.342	0.035	0.611	53	20.85	20.08	25.90	89.71	1.53	393
27-July[1]	5:01−9:05	58.0	0.43	−57.6	0.221	0.043	0.98	14	23.77	24.29	25.21	78.42	2.39	377
1-Aug[2]	8:35−11:45	122	33.8	−87	1.262	0.246	−0.62	0	30.68	34.21	26.76	56.61	2.81	148
1-Aug[3]	12:10−15:04	101	33.8	−68.5	1.725	0.307	−0.277	0	33.60	37.28	29.61	40.29	1.08	41

[a] Positive and negative fluxes are defined as net emissions and depositions respectively. [1,2,3] Profile categories 1, 2, and 3 from the text, respectively.

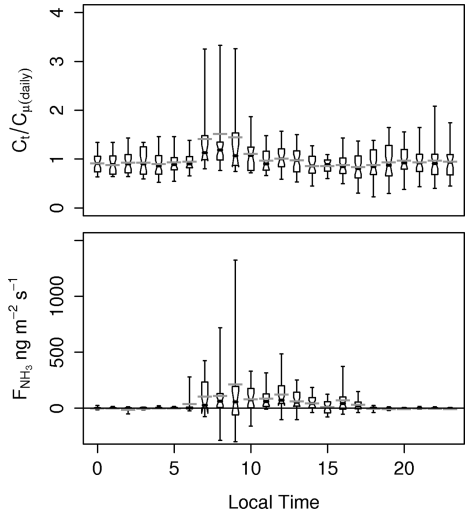

FIGURE 5. Box plots and mean (gray bar) and whiskers represent the 5th and 95th percentile of the mean diurnal hourly concentration, C_t, normalized by the mean daily concentration, $C_{\mu(daily)}$, $z = 1$ m (top panel) and above-canopy MBR NH_3 flux estimates. Positive values indicate emissions and negative values indicate deposition (bottom panel) from July 6th through August 1st. The notches are the asymptotic normality of the median and represent the 95% confidence interval for the difference in two medians.

sources. This simple model lacks the sophistication of higher order Eulerian closure and LNF models but estimated canopy and soil sources and sinks agree reasonably well when a strong monotonic in-canopy concentration profile is present. Furthermore, the model presented here may be used to parameterize in-canopy resistances and to constrain canopy and soil NH_3 partitioning suitable for air-quality model air surface exchange algorithms. As expected, model performance was poorest when there were weak nonmonotonic scalar concentration profiles within the canopy (discussed in SI Text S1), particularly during morning and evening transition periods when flow is nonstationary. The results obtained using this technique are being used in conjunction with measurements of soil, apoplast and vegetation surface chemistry, and canopy structural and physiological parameters to refine the bidirectional NH_3 surface exchange model currently in development for the community multiscale air quality (CMAQ) model (*49*).

Acknowledgments

G.K. acknowledges support from the National Science Foundation (NSF-EAR 06-35787, NSF-EAR-06-28432, and NSF-ATM-0724088), and the Binational Agricultural Research and Development (BARD, Research Grant No. IS3861-06). This work was funded by USDA CSREES Air Quality Program Grant No. 35112 and U.S. EPA Office of Research and Development. Although this work was reviewed by EPA and approved for publication, it may not necessarily reflect official Agency policy. Mention of commercial products does not constitute endorsement by the Agency.

Supporting Information Available

Additional information on the assumptions and applicability of the first order closure model. This material is available free of charge via the Internet at http://pubs.acs.org.

Literature Cited

(1) Pope, C. A.; Dockery, D. W. Health effects of fine particulate air pollution: Lines that connect. *J. Air Waste Manage. Assoc.* **2006**, *56*, 709–742.

(2) Sutton, M. A.; Nemitz, E.; Erisman, J. W.; Beier, C.; Bahl, K. B.; Cellier, P.; de Vries, W.; Cotrufo, F.; Skiba, U.; Di Marco, C.; et al. Challenges in quantifying biosphere-atmosphere exchange of nitrogen species. *Environ. Pollut.* **2007**, *150*, 125–139.

(3) Vitousek, P. M.; Aber, J. D.; Howarth, R. W.; Linkens, G. E.; Matson, P. A.; Schindler, D. W.; Schlesinger, W. H.; Tilman, D. G. Human alteration of the global nitrogen cycle: Sources and consequences. *Ecol. Appl.* **1997**, *7* (3), 737–750.

(4) Sutton, M. A.; Asman, W. A. H.; Schjørring, j.K. Dry deposition of reduced nitrogen. *Tellus* **1994**, *46*, 255–273.

(5) Erisman, J. W.; Sutton, M. A.; Galloway, J.; Klimont, Z.; Winiwarter, W. How a century of ammonia synthesis changed the world. *Nat. Geosci.* **2008**, *1*, 636–639.

(6) Teye, F. K.; Hautala, M. Adaption of an ammonia volatilization model for a naturally ventilated dairy building. *Atmos. Environ.* **2008**, *42*, 4345–4354.

(7) Sutton, M. A.; Schjørring, J. K.; Wyers, G. P. Plant-atmosphere exchange of ammonia. *Philos. Trans. R. Soc., A* **1995**, *351*, 261–278.

(8) Massad, R. S.; Loubet, B.; Tuzet, A.; Cellier, P. Relationship between ammonia stomatal compensation point and nitrogen metabolism in arable crops: Current status of knowledge and potential modeling approaches. *Environ. Pollut.* **2008**, *154*, 390–403.

(9) Holland, E. A.; Braswell, B. H.; Sulzman, J.; Lamarque, J.-F. Nitrogen deposition onto the United States and Western Europe:

Synthesis of observations and models. *Ecol. Appl.* **2005**, *15* (1), 38–57.
(10) Sutton, M. A.; Burkhardt, J. K.; Guerin, D.; Nemitz, E.; Fowler, D. Development of resistance models to describe measurements of bi-directional ammonia surface atmosphere exchange. *Atmos. Environ.* **1998**, *32*, 473–480.
(11) Nemitz, E.; Milford, C.; Sutton, M. A. A two-layer canopy compensation point model for describing bi-directional biosphere-atmosphere exchange of ammonia. *Q. J. R. Meterol. Soc.* **2001**, *127*, 815–833.
(12) Jones, M. R.; Raven, J. A.; Leith, I. D.; Cape, J. N.; Smith, R. I.; Fowler, D. Short-term flux chamber experiment to quantify the deposition of gaseous ^{15}N-NH_3 to *Calluna vulgaris*. *Agric. For. Meteorol.* **2008**, *148* (6−7), 893–901.
(13) Walker, J. T.; Robarge, W. P.; Wu, Y.; Meyers, T. P. Measurements of bi-directional ammonia fluxes over soybean using the modified Bowen-ratio technique. *Agric. For. Meteorol.* **2006**, *138*, 54–68.
(14) Wyers, G. P.; Otyes, R. P.; Slanina, J. A continuous-flow denuder for the measurement of ambient concentrations and surface exchange of ammonia. *Atmos. Environ.* **1993**, *27A*, 2085–2090.
(15) Nemitz, E.; Flynn, M.; Williams, P. I.; Milford, C.; Theobald, M. R.; Blatter, A.; Ballagher, M. W.; Sutton, M. A. A relaxed eddy accumulation system for the automated measurement of atmospheric ammonia fluxes. *Water, Air, Soil Pollut.* **2001**, *1* (5−6), 189–202.
(16) Hensen, A.; Nemitz, E.; Flynn, M. J.; Blatter, A.; Jones, S. K.; Sørensen, L. L.; Hensen, B.; Pryor, S.; Jensen, B.; Otjes, R. P.; Sutton, M. A. Inter-comparison of ammonia fluxes obtained using the eddy accumulation technique. *Biogeosciences Discuss.* **2008**, *5*, 3965–4000.
(17) Whitehead, J. D.; Twigg, M.; Famulari, D.; Nemitz, E.; Sutton, M. A.; Gallagher, M. W.; Fowler, D. Evaluation of laser absorption spectroscopic techniques for eddy covariance flux measurements of ammonia. *Environ. Sci. Technol.* **2008**, *42*, 2041–2046.
(18) Denmead, O. T.; Freney, J. R.; Dunin, F. X. Gas exchange between plant canopies and the atmosphere: case-studies for ammonia. *Atmos. Environ.* **2008**, *42*, 3,394–3,406.
(19) Nemitz, E.; Sutton, M. A.; Gut, A.; San José, R.; Husted, S.; Schjørring, J. K. Sources and sinks of ammonia within an oilseed rape canopy. *Agric. For. Meteorol.* **2000**, *105* (4), 385–404.
(20) Nemitz, E.; Loubet, B.; Lehmann, B. E.; Cellier, P.; Neftel, A.; Jones, S. K.; Hensen, A.; Ihly, B.; Tarakanov, S. V.; Sutton, M. A. Turbulence characteristics in grassland canopies and implications for tracer transport. *Biogeoscie. Discuss.* **2009**, *6*, 437–489.
(21) Harper, L. A.; Sharpe, R. R. Nitrogen dynamics in irrigated corn - soil-plant nitrogen and atmospheric ammonia transport. *Agron. J.* **1995**, *87* (4), 669–675.
(22) Katul, G. G.; Albertson, J. D. Modeling CO_2 sources, sinks, and fluxes within a forest canopy. *J. Geophys. Res.* **1999**, *104* (6), 6081–6091.
(23) Siqueira, M.; Katul, G. G.; Lai, C.-T. Quanitfying net ecosystem exchange by multilevel ecophysiological and turbulent transport models. *Adv. Water Resour.* **2002**, *25*, 1357–1366.
(24) Siqueira, M.; Lai, C.-T.; Katul, G. G. Estimating scalar sources, sinks and fluxes in a forest canopy using Lagrangian, Eulerian, and hybrid inverse models. *J. Geophys. Res.* **2000**, *105* (24), 29475–29488.
(25) Siqueira, M.; Leuning, R.; Kolle, O.; Kelliher, F. M.; Katul, G. G. Modelling sources and sinks of CO_2, H_2O and heat within a Siberian pine forest using three inverse methods. *Q. J. R. Meterol. Soc.* **2003**, *129* (590), 1373–1393.
(26) Siqueira, M.; Katul, G. G. Estimating heat sources and fluxes in thermally stratified canopy flows using higher-order closure models. *Boundary Layer Meteorol.* **2002**, *103*, 125–142.
(27) Cava, D.; Katul, G. G.; Scrimieri, A.; Poggi, D.; Cescatti, A.; Giostra, U. Buoyancy and the sensible heat flux budget within dense canopies. *Boundary Layer Meteorol.* **2006**, *118*, 217–240.
(28) Juang, J.-Y.; Katul, G. G.; Siqueira, M. B.; Stoy, P. C.; Palmroth, S.; McCarthy, H. R.; Kim, H. S.; Oren, R. Modeling nighttime ecosystem respiration from measured CO_2 concentration and air temperature profiles using inverse methods. *J. Geophys. Res.* **2006**, *111*, D08S05.
(29) Raupach, M. R. A practical Lagrangian method for relating scalar concentrations to source distributions in vegetation canopies. *Q. J. R. Meterol. Soc.* **1989**, *115*, 609–32.
(30) Katul, G. G.; Oren, R.; Ellsworth, D.; Hsieh, C. I.; Phillips, N.; Lewin, K. A Lagrangian dispersion model for predicting CO_2 sources, sinks, and fluxes in a uniform loblolly pine; (*Pinus taeda L.*) stand. *J. Geophys. Res.* **1997**, *102*, 9309–9321.
(31) Leuning, R.; Denmead, O. T.; Miyata, A.; Kim, J. Source/sink distributions of heat, water vapour, carbon dioxide and methane in a rice canopy estimated using Lagrangian dispersion analysis. *Agric. For. Meteorol.* **2000**, *104*, 233–249.
(32) Harman, I. N.; Finnigan, J. J. Scalar concentration profiles in the canopy and roughness sublayer. *Boundary Layer Meteorol.* **2008**, *129*, 323–351.
(33) Husted, S.; Schjoerring, J. K. Ammonia flux between oilseed rape plants and the atmosphere in response to changes in leaf temperature, light intensity, and air humidity. *Plant Physiol.* **1996**, *112*, 67–74.
(34) Harman, I. N.; Finnigan, J. J. A simple unified theory for flow in the canopy and roughness sublayer. *Boundary Layer Meteorol.* **2007**, *123*, 339–363.
(35) Finnigan, J. Turbulence in plant canopies. *Annu. Rev. Fluid Mech.* **2000**, *32*, 519–571.
(36) Katul, G. G.; Mahrt, L.; Poggi, D.; Sanz, C. One- and two-equation models for canopy turbulence. *Boundary Layer Meteorol.* **2004**, *113*, 81–109.
(37) Inoue, E. On the turbulent structure of air flow within crop canopies. *J. Meteorol. Soc. Japan* **1963**, *41*, 317–326.
(38) Byun, D. W. On the analytical solution to the flux-profile relationships for the atmospheric surface layer. *J. Appl. Meteor.* **1990**, *29*, 652–657.
(39) Wilson, J. D. A 2nd order closure model for flow through vegetation. *Boundary-Layer Meteorol.* **1988**, *42*, 371–392.
(40) Yi, C. Momentum transfer within canopies. *J. Appl. Meteor. Clim.* **2008**, *47*, 262–275.
(41) Poggi, D.; Porporato, A.; Ridolfi, L.; Albertson, J. D.; Katul, G. G. The effect of vegetation density on canopy sub-layer turbulence. *Boundary-Layer Meteorol.* **2004**, *111*, 565–587.
(42) Harper, L. A.; Denmead, O. T.; Sharpe, R. R. Identifying sources and sinks of scalars in a corn canopy with inverse Lagrangian dispersion analysis II. Ammonia. *Agric. For. Meteorol.* **2000**, *104*, 75–83.
(43) Walker, J. T.; Jones, M. R.; Bash, J. O.; Myles, L.; Luke, W.; Meyers, T. P.; Robarge, W.; Air surface exchange of ammonia in a fertilized corn canopy from planting through senescence. In preparation.
(44) Roelle, P. A.; Aneja, V. P. Characterization of ammonia emissions from soils in the upper coastal plain, North Carolina. *Atmos. Environ.* **2002**, *36*, 1087–1097.
(45) Jones, M. R.; Leith, I. D.; Fowler, D.; Raven, J. A.; Sutton, M. A.; Nemitz, E.; Cape, J. N.; Sheppard, L. J.; Smith, R. I.; Theobald, M. R. Concentration-dependent NH_3 deposition processes for mixed moorland semi-natural vegetation. *Atmos. Environ.* **2007**, *41* (10), 8980–8994.
(46) Wilson, J. D.; Flesch, T. K. Flow boundaries in random-flight dispersion models: enforcing the well-mixed condition. *J. Appl. Meteorol.* **1993**, *32*, 1695–1707.
(47) Sommer, S. G.; Schjoerring, J. K.; Denmead, O. T. Ammonia emissions from mineral fertilizers and fertilized crops. *Advanc. Agron.* **2004**, *82*, 557–622.
(48) Sommer, S. G.; Friis, E.; Bach, A.; Schjørring, J. K. Ammonia volatilization from pig slurry applied with trail hoses or broadspread to winter wheat: effects of crop development stage, microclimate, and leaf ammonia absorption. *J. Environ. Qual.* **1997**, *26*, 1153–1160.
(49) Byun, D.; Schere, K. L. Review of the governing equations, computational algorithms, and other components of the Models-3 Community Multiscale Air Quality (CMAQ) modeling system. *Appl. Mech. Rev.* **2006**, *59*, 51–77.

ES9037269